Materials International
Open-Access Journal (ISSN: 2668-5728)

Article
Volume 7, Issue 4, 2025, 39
https://doi.org/10.33263/Materials74.039

The Effects of Incorporating POT-MWCNT into PEDOT: PSS on the Performance of OFET

Manal Z. Rajab [1], Kareema M. Ziadan [2]

[1] Department of Physics, College of Science, University of Basrah, Basrah, Iraq; manal.zeki@uobasrah.edu.iq (M.Z.R.); kareema.ziadan@uobasrah.edu.iq (K.M.Z.);
* Correspondence: manal.zeki@uobasrah.edu.iq;

Received: 29.06.2025; Accepted: 29.10.2025; Published: 10.12.2025

Abstract: The mixture of poly(3,4-ethylenedioxythiophene): polystyrene sulfonate (PEDOT: PSS) with poly(o-toluidine)-multi-walled carbon nanotube (POT: MWCNT) composites results in a distinctive hybrid material system for organic field-effect transistor (OFET) applications. This mixture leverages the synergistic properties of all three constituents (PEDOT:PSS, POT, and MWCNTs) to improve device performance. To the best of our knowledge, this is the first study to integrate POT–MWCNT composites into the PEDOT: PSS matrix as a hybrid active layer for OFETs. This unique combination aims to synergistically enhance charge mobility and interfacial stability beyond what has been achieved with conventional single-polymer or nanotube-doped systems.MWCNTs facilitate one-dimensional conduction channels within the polymer matrix, whereas POT's extended π-conjugation promotes intermolecular hopping, and PEDOT: PSS occupies vacancies in the MWCNT network. The electrical characterization is performed at V_{GS} ranging from -25 to 25 and V_{DS} from -1 to -30 over five sweeps for bottom-contact OFETs fabricated with the optimized (PEDOT: PSS) + POT: MWCNT. The Source/Drain electrodes exhibited a field-effect mobility of 5.01 cm²/(V·s), utilizing polyvinyl alcohol as the gate dielectric. Critical device parameters (mobility, threshold voltage, on/off current ratio, etc.) are computed. The superior device at V_{DS} = -6.75 volts. This hybrid material shows great potential for use in flexible electronics, smart sensors, and next-generation wearable devices.

Keywords: organic field effect transistor; charge carrier mobility; blending polymers; MWCNT.

1. Introduction

Organic field-effect transistors are innovative devices, and multi-component blend systems provide a crucial solution to the significant challenges faced in advancing OFETs. Organic multi-component systems are analogous to alloys and electronics, in which the active semiconducting layer is composed of π-conjugated organic small molecules and polymers [1]. OFETs derive substantial advantages from the incorporation of PEDOT: PSS (poly(3,4-ethylenedioxythiophene): polystyrene sulfonate) combined with POT: MWCNT (poly(o-toluidine)-multi-walled carbon nanotube composites). This hybrid solution improves charge transport, interfacial properties, and device stability, making it suitable for flexible and printed electronics [2,3]. Improved Charge Transport and Conductivity PEDOT: PSS offers elevated electrical conductivity, reaching up to 1000 S/cm with the addition of supplementary dopants such as DMSO or EG [4]. Creates a continuous conductive matrix that stabilizes charge transport, stops current leakage, and increases hole transport and film uniformity through

solution-processability[5]. Doping modification is made easier by POT's (poly(o-toluidine)) adjustable redox activity. It is more compatible with organic semiconductors due to its conjugated structure. In comparison to pure PEDOT: PSS, improved mechanical flexibility [6].

MWCNTs create percolation pathways, reduce the conductivity threshold, and increase charge-carrier mobility (due to ballistic electron transport along nanotubes). In flexible organic field-effect transistors (OFETs), mechanical strength offers high-mobility paths that enhance field-effect mobility (μFET) and prevent crack formation [7,8]. Synergistic Impacts PEDOT: PSS reduces contact resistance by filling up gaps in the MWCNT network. By reducing grain boundaries and trap states, POT acts as a dispersion to improve blend homogeneity, prevent MWCNT aggregation, and improve film form[9]. The combined effect of polymers attains superior conductivity compared to each component, resulting in diminished series resistance in OFET electrodes [10]. At the semiconductor/dielectric interface, the persistent dipole generates an energy barrier to charge transfer. By raising the dielectric's HOMO energy, a fluorinated polymer at the semiconductor/dielectric interface can improve the energetic barrier for charge transfer from the semiconductor to the dielectric (charge trapping)[11].

To enhance their physical and chemical properties over a single metal, metals are combined with metallic or nonmetallic substances. Similarly, single-component semiconductor materials can exhibit limited performance and are difficult to obtain simultaneously, despite high expectations for high-performance OFETs. Consequently, materials scientists are now concentrating on multi-component systems. This might expedite the advancement of organic transistors. In addition, several organic optoelectronic devices have adopted multi-component mix systems, including organic photovoltaic cells and organic light-emitting diodes, and have advanced significantly [12,13]. Incorporating high-molecular-weight polystyrene (PS) into the organic semiconductor (OSC) markedly affects the spatial confinement of the dopant within the device. This method is essential for regulating dopant diffusion into the organic semiconductor, a prevalent challenge in organic field-effect transistors [14].

Solution-processed π-conjugated semiconductive and conductive molecules represent the most promising candidate materials for the fabrication of printed and flexible electronics due to their numerous advantages over inorganic counterparts, including low-temperature processing, exceptional mechanical compatibility resulting from their high bendability and stretchability, and the potential for precise modulation of the materials' electrical properties through molecular functionalization [15].

PVA-based OFETs frequently exhibit lower field-effect mobility (lFE) and significant drain current (IDS) hysteresis, which may be linked to factors such as the polar interface near the conducting channel [16]. The substantial OH-groups on the PVA surface and the mobile ions within the PVA bulk [17]. Carbon-based materials, including graphene and carbon nanotubes (CNTs), exhibit significant potential for flexible electronics due to their inherent high mobility and mechanical flexibility [18].

Covalent functionalization of carbon nanotubes enhances their solution dispersibility and compatibility with organic semiconductors [19]. A specific variant of carbon nanotubes is two concentrically aligned single-walled carbon nanotubes (SWCNTs) that make up a multi-walled carbon nanotube (MWCNT) [20].

This study presents a composite of a conducting polymer blended with MWCNT and another polymer, examining its impact on OFET performance, including mobility, current density, threshold voltage, and more. Incorporating f-MWCNT into organic semiconductors significantly enhances the electrical performance of the OFET. The

PEDOT:PSS+POT:MWCNT hybrid system represents a significant advancement in organic electronics, combining solution-processability with improved electrical performance and environmental stability for future OFET applications.

2. Materials and Methods

PEDOT: PSS 99% from Sigma-Aldrich, poly(vinyl alcohol) (PVA) was purchased from Sigma Aldrich, (Mw = 89,000 – 98,000 99+% hydrolysis), OT-monomers 99% from Fisher Scientific, hydrochloric acid 99.9% Fluka, ammonium per sulphate, purity 98%, ethanol purity 99.9%, Scharlau, MWCNT purity 95%, DMSO, dimethyl sulfoxide $(CH_3)_2SO$, Mw 78.13, puriss. p.a., ACS reagent, ≥99.9% (GC) from Sigma-Aldrich.

The Ossila pre-patterned ITO Glass Substrates, 20 x 15 mm, OFET sensing substrate, and its board are used as shown in Figure 1a. Product Code S161 is designed to allow the fabrication and characterization of transistors. The OFET Test Board, as shown in Figure 1 b.

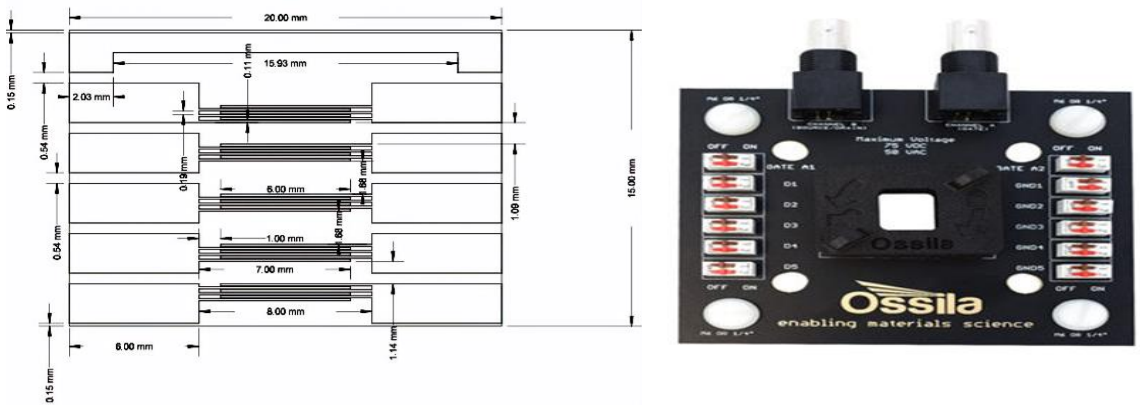

(a) **(b)**

Figure **1. (a)** Ossila ITO OFET substrate; **(b)**The OFET test board.

2.1. OFET fabrication.

The OFET substrate was placed in an ultrasonic bath containing DI water for 10 minutes; after that, acetone was removed by ultrasonication for 10 minutes, and the substrate was then placed in the oven at 40ºC, where the active materials solution was deposited, followed by the dielectric layer. A diagram showing the arrangement of the material layers in the device is shown in Figure 2

The conducting polymer (POT-HCl) was prepared by chemical polymerization from the monomer o-toluidine. The Ammonium persulfate (APS) is used as an oxidizing agent. O-Toluidine monomer was dissolved in 10 mL (1M/HCl), then APS was added to it under constant mechanical stirring at (0-5ºC). The reaction was put under a magnetic stirrer for 24 h. Finally, the resulting powder is a dark green color. The blending (POT**:**MWCNT+PEDOT: PSS) active layer is made by spin-coating at 1500 rpm for 60 sec. The created film was dried in the oven for an hour at 40°C and then raised to 60°C for 30 minutes. The conducting polymer POT /HCl 0.1g was dissolved in DMSO (5ml). This POT/HCl blend includes 5% MWCNT that has been ultrasonically sonicated and then blended with PEDOT: PSS pure, remained on the magnetic stirrer for 3 hours, and then blended with PEDOT: PSS by direct mixing [21].

Polyvinyl alcohol (PVA) was weighed, dissolved in 10 mL of deionized water, mechanically stirred for two hours at 80°C, and filtered using a 0.22 µm filter syringe. The

insulating polymer film was also made by spin-coating and dried in an oven for 3 hours at 30 or 1500 rpm.

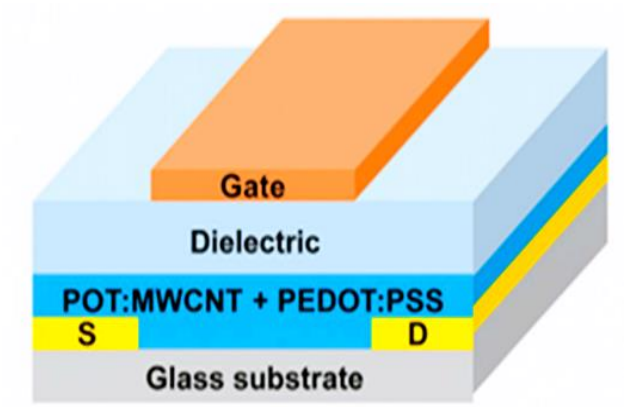

Figure 2. Schematic of an OFET top-gate bottom-contact.

2.2. Physical characterization.

2.2.1. FE-SEM for POT:MWCNT+PEDOT:PSS.

Blending this POT: MWCNT composite with PEDOT: PSS further enhances the film's mechanical flexibility, surface smoothness, and stability. PEDOT: PSS acts as a secondary conducting polymer and dispersing agent, improving film formation and maintaining high conductivity even at lower processing temperatures. The sulfonate groups of PSS can also facilitate protonic doping of POT, which contributes to higher charge carrier mobility [21]. As shown in Figure 3.

Morphologically, SEM micrographs typically show a porous and interconnected network with nanofiber-like or granular structures, indicating good integration of the three components. The resulting hybrid structure combines the chemical stability and processability of PEDOT:PSS, the electroactivity of POT, and the electronic conductivity of MWCNTs, making it a promising candidate for applications in organic field-effect transistors (OFETs), chemical sensors, and energy storage devices.

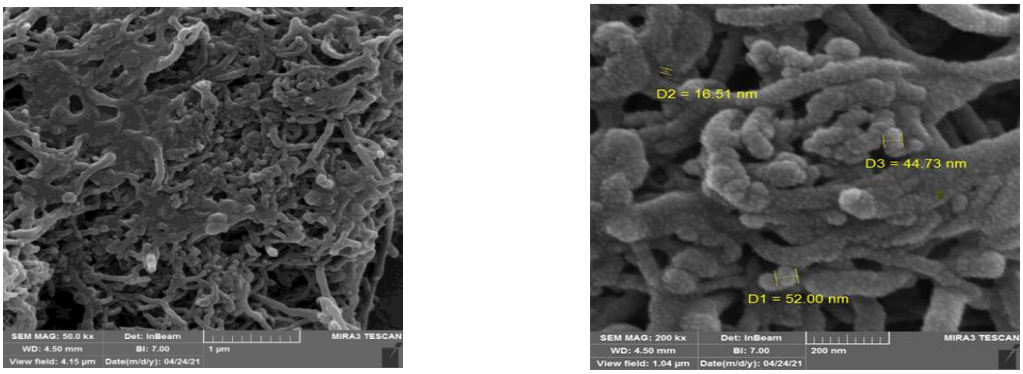

(a) **(b)**

Figure 3. FE-SEM micrograph of blend POT:MWCNT+PEDOT: PSS.

3. Results and Discussion

3.1. Output characteristics.

A P-type field effect transistor (POT: MWCNT/PEDOT: PSS-OFET) was fabricated using pure polymers. The insulating layer thickness was 1500 rpm, the conducting channel width was 30 mm, and the channel length was 50 μm.

The PVA films' minimal thickness and elevated dielectric constant enabled the low-voltage operation. Significant leakage currents were observed in all devices using pristine PVA as the dielectric layer. The mobility of the charge carriers was assessed in both the linear and saturation zones, as indicated by the two equations below (1,2). The channel length, L, is 50 μm, the channel width, W, is 30 mm, and the capacitance of the insulating layer, Ci, is defined by the relationship with capacitance in nano farads. The frequency in kilohertz, by inserting equations (3, 4), we determined the value of mobility [22], which is equations (3) and (4):

Ids, Lin $V_{DS} << V_{GS}-V_{th}$

$$I_{DS,Lin}=\frac{W\mu C_i}{L}(V_{GS}-V_{th})V_{DS} \quad (1)$$

if ($V_{DS}<<V_{GS}-V_{th}$)

Ids, sat $V_{DS} > V_{GS}-V_{th}$.

$$I_{DS,sat}=\frac{W\mu C_i}{2L}(V_{GS}-V_{th})^2 \quad (2)$$

if ($V_{DS} > V_{GS}-V_{th}$)

According to the two equations above, the mobility of the charge carriers was calculated in the linear region and the saturation region by substituting the equations. (2), (1) we found the value of mobility, which is:

$$\mu_{Lin}=\frac{L}{WC_i V_{DS}}\left(\frac{\partial I_{DS}}{\partial V_{GS}}\right) \quad (3)$$

$$\mu_{sat}=\frac{2L}{WC_i}\left(\frac{\sqrt{\partial I_{DS}}}{\partial V_{GS}}\right)^2 \quad (4)$$

The fluctuation rate of I_{DS} in decades concerning V_{GS} for a device functioning in the sub-threshold region is called the sub-threshold slope (SS). As the current increases, the value of SS is obtained by applying a linear fit to the logarithm of Ids, revealing a value of 12 V/dec. The mathematical formula for the sub-threshold slope is shown in. The sub-threshold swing quantifies the rate at which the device activates, indicated by the increase in drain current (I_{DS}) relative to gate-source voltage (V_{GS}), with a lower value signifying superior device performance. Values of 0.88 V/dec were estimated for pentacene Thin Film Transistors utilizing Cytop dielectric, while 0.1 V/dec was seen with a Self-assembled mono layer (SAM) dielectric.

$$SS=\frac{\partial[V_{GS}]}{\partial[Log_{10}I_{DS}]} \quad (5)$$

g_m denotes "trans-conductance." These equations disregard the influence of traps and parasitic resistances as they do not account for gate-voltage-dependent mobility. An augmentation in the drain current I_D with heightened negative gate-source voltage V_{GS} denotes a hole-transporting organic layer. In an electron-transporting material, the drain current rises with the application of a positive gate-source voltage, but in the case of ambipolar transport, the current increases for both positive and negative voltages [23].

$$g_m=\left(\frac{\partial I_d}{\partial V_G}\right)_{V_D=constant}=\frac{WC_i}{L}\mu_{FET}V_{DS} \quad (6)$$

The resistance in an organic field effect transistor can be calculated from the relationship and the output characteristics, as shown in Table 1.

$$R = \left(\frac{\partial I_d}{\partial V_D} \right)_{V_G = constant} \quad (7)$$

Figure 4 shows the output characteristic (source-drain) as a function of the negative voltage (source-drain) for all values of gate voltage V_{GS}=25, 12.5, 0.12.5, -25 volts. It can be seen from the Figure that the I_{DS} increases with an increase in the negative voltage V_{DS}, and this increase is linear and subject to Ohm's law until the pinch-off point. This ohmic behavior continues until the saturation state is reached, after which the source-drain current conductance becomes almost constant with increasing source-drain voltage for all values of applied gate voltage. The polyethylenedioxythiophene (PEDOT) chain is rich with holes and then doped with polystyrene sulfonate (PSS) with sulfonate anions that compensate for these holes. According to the literature, PEDOT: PSS is conductive (p-type) in its initial state (i.e., no gate voltage is applied). This confuses me because I would have thought compensating these holes by adding PSS would have made the PEDOT less conductive.

Figure 4 describes the relation between Drain-Source current (I_{DS}) versus Drain-Source voltage (V_{DS}) for this device's Organic field effect transistor with different V_{GS}. High saturation levels at V_{DS}=-13 V and the contact resistance (R) were determined from the linear region of I_{DS}-V_{DS} with constant V_{GS}, where it decreases with decreased V_{GS}. Figures 4 and 5 show the transfer characteristics of the OFET device. This is represented by the relation between Ids versus V_{GS} from the voltages (-25 → 25) Volt at different V_{DS} (0 → -30) V. The Current I_{DS} were increased with decreased V_{DS}, and the tars-conductance (g_m) appeared semi-stable with decreased V_{DS}, where it changed between 2.2×10^{-2} → 1.2×10^{-1} S.

Table 1. Device parameters OFET of PEDOT: PSS+POT/HCl based devices (L=50µm, W=30mm).

V_{DS}	V_{th} (V)	I_{on}/I_{off}	μ_{Lin} (cm^2/Vs)	μ_{sat} (cm^2/Vs)	g_m (S)	V_0 (V)	SS (V/dec)
V_{DS}=-30	1.9	1.02×10^{2}	4.003	5.01	1.2×10^{-1}	24.8	1.1×10^{-2}
V_{DS}=-22.25	3.8	1.2×10^{2}	2.17	3.59	1.15×10^{-1}	25.06	1.2×10^{-2}
V_{DS}=-14.5	2.7	1.0×10^{2}	6.7×10^{-1}	3.2×10^{-2}	9.8×10^{-2}	24.2	1.2×10^{-3}
V_{DS}=-6.75	1	1.3×10^{3}	3.6	4.53	2.2×10^{-2}	24.6	2.3×10^{-4}

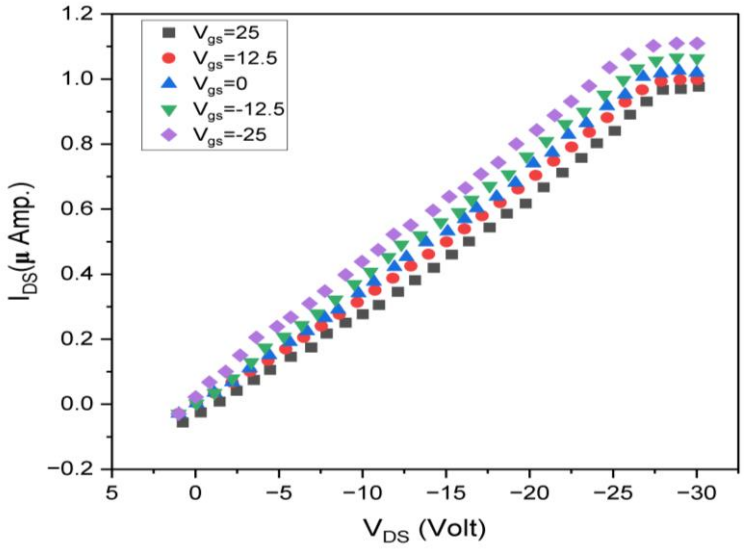

Figure 4. Output characteristic of PEDOT: PSS+POT-HCl/MWCNT based OFET (L=50 µm, W=30 mm).

The mobility of the charge carriers in the linear region and the saturation region was calculated from the slope of the tangent straight line in Figure 5 by taking advantage of relations

(3), (4), (5), and (6). The straight-line extension along the V_{GS} axis also found the threshold voltage. The ratio between the on and off currents, I_{on}/I_{off}, was also calculated from the highest and lowest values in Figure 6.

The device was evaluated for drain-source voltages (V_{DS}) between (-1→-30) V, and gate-source voltages (V_{GS}) between (-25 → 25)V. Their electrical parameters are in Table 1.

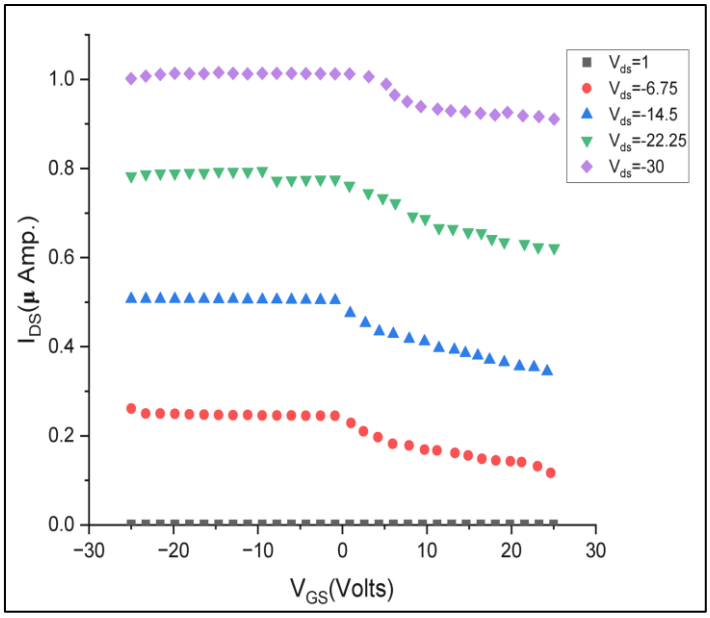

Figure 5. Transfer curves of OFET (ITO/PEDOT: PSS+POT-HCl/MWCNT/PVA/Al).

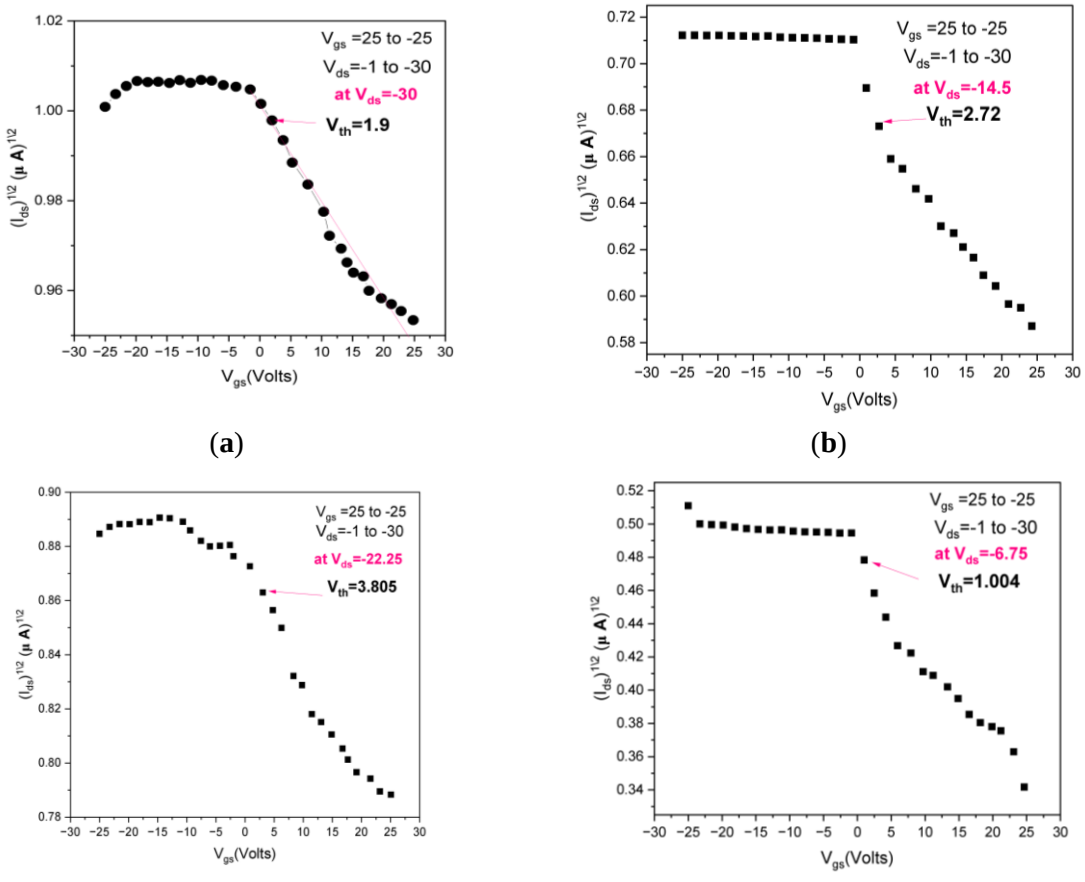

Figure 6. The square root as a function of for OFET with different V_{DS}.

The electrical performance of the fabricated OFET based on POT blended with MWCNT and PEDOT: PSS shows a noticeable enhancement compared to devices reported in previous studies using pure conducting polymers. The incorporation of MWCNTs within the POT matrix significantly improves the charge carrier mobility due to the formation of additional conductive pathways that facilitate electron transport. Furthermore, the addition of PEDOT: PSS enhances the interfacial contact and film uniformity, leading to a more stable current–voltage behavior. Although the on/off current ratio obtained in this study is slightly lower than that reported in previous studies, the charge-carrier mobility shows a clear improvement. The reduction in the on/off ratio may be attributed to increased leakage current due to the presence of MWCNTs, which provide additional conductive pathways even in the off-state. However, the same conductive network significantly enhances charge transport in the active layer, resulting in higher mobility than similar OFETs based on POT or PEDOT: PSS alone. These findings suggest that while introducing MWCNTs improves carrier transport properties, further optimization of the device structure or the dielectric interface is required to balance the trade-off between mobility and on/off ratio. The data in Table 1 indicate that mobility in the saturation zone exceeds that in the linear region. This indicates that the transistor has superior current transfer efficiency at elevated operating voltages. This behavior results from multiple physical phenomena within the OFET, including lower resistance or enhanced conductivity compared to the results reported by Prasanta Ghosh [23,24].

The on-off current ratio at a voltage of V_{DS} = -6.75 is 1.3 × 10^3, representing the optimal value, and remains nearly steady across all voltage levels. The transistor may alternate between the on and off states with average efficiency. The sub-threshold voltage (SS) quantifies the efficiency of a transistor in transitioning between its on and off states. A lower slope value indicates superior current control by the organic field effect transistor, resulting in reduced power consumption and diminished current leakage in the off state. In this study, at V_{DS} = -6.75, the value is 2.3×10^{-4} V/dec.

As shown in Table 2, in an organic field-effect transistor (OFET) application, negative resistance corresponds to negative differential resistance (NDR). This does not imply that the material exhibits negative resistance in the conventional sense (where current increases as voltage decreases); instead, it indicates that, within a particular segment of the current-voltage (I-V) curve, an increase in the applied voltage leads to a decrease in the current through the device. Pinch-off or saturation: In field-effect transistors, when the drain-to-source voltage (V_{DS}) reaches a specific value (the saturation voltage), the conduction channel begins to "pinch" or narrow near the drain terminal. Any further increase in V_{DS} after this point does not result in a significant increase in the drain current (I_{DS}). In some cases, complex events such as oversaturation or the introduction of opposing charge carriers can result in a slight decrease in current.

Table 2. Shows the OFET device parameter for resistance as a function of gate-source voltage.

V_{GS}(Volt)	R (Ω)
25	-30.85
12.5	-28.7
0	-27.5
-12.5	-25.95
-25	-24.22

Mechanisms for trapping and untrapping: Organic materials have a variety of deep energy levels that can trap charge carriers, such as electrons or holes. When a specific voltage is applied, these sites may become more effective at trapping charge carriers, reducing the

number of free charge carriers available for conduction, and lowering the current as the voltage rises. Interface Effects: The appearance of negative differential resistance (NDR) may be affected by contact between an organic semiconductor and an insulator or between a semiconductor and a metal (electrodes) [25].

4. Conclusions

Organic field-effect transistors (OFETs) with PEDOT: PSS and POT: MWCNT composites have significantly improved a number of electrical characteristics. In comparison to traditional polymer systems, these hybrid materials improve charge carrier mobility and conductivity by utilizing the unique properties of each component. Multi-walled carbon nanotubes (MWCNTs) effectively overcome the limitations typically encountered by conventional organic semiconductors by creating one-dimensional conduits that improve charge transfer. The poly(o-toluidine) conjugated with π (POT) architecture is essential for this composite material's charge transport kinetics. Moreover, experimental findings demonstrate a significant enhancement in electrical conductivity and mobility inside these composites, improving overall performance. This development underscores the substantial potential of integrating conductive polymers with nanomaterials, such as MWCNTs, to markedly enhance the performance attributes of OFETs.

Author Contributions

Conceptualization, M.Z.R. and Y.Y.; methodology, K.Z.M.; software, M.Z.R.; validation, M.Z.R. and K.Z.M.; formal analysis, M.Z.R.; investigation, M.Z.R.; resources, M.Z.R.; data curation, M.Z.R.; writing—original draft preparation, M.Z.R.; writing—review and editing, M.Z.R.; visualization, M.Z.R.; supervision, K.Z.M.; project administration, X.X.; funding acquisition, Y.Y. All authors have read and agreed to the published version of the manuscript.

Funding

This research received no external funding.

Acknowledgments

The practical part of the work was completed at the University of Basrah, College of Science, Department of Physics, in the Conductive Polymer Electronics Research Laboratory, and in System Lab View 2018.

Conflicts of Interest

The authors declare no conflict of interest. The funders had no role in the design of the study; in the collection, analyses, or interpretation of data; in the writing of the manuscript, or in the decision to publish the results.

References

1. Kim, Y.; Chung, S.; Cho, K.; Harkin, D.; Hwang, W.-T.; Yoo, D.; Kim, J.-K.; Lee, W.; Song, Y.; Ahn, H.; Hong, Y.; Sirringhaus, H.; Kang, K.; Lee, T. Enhanced Charge Injection Properties of Organic Field-Effect Transistor by Molecular Implantation Doping. *Advanced Materials* **2019**, *31*, 1806697, https://doi.org/10.1002/adma.201806697.

2. Lin, D.; Zhang, W.; Yin, H.; Hu, H.; Li, Y.; Zhang, H.; Wang, L.; Xie, X.; Hu, H.; Yan, Y.; Ling, H.; Liu, J.a.; Qian, Y.; Tang, L.; Wang, Y.; Dong, C.; Xie, L.; Zhang, H.; Wang, S.; Wei, Y.; Guo, X.; Lu, D.; Huang, W. Cross-Scale Synthesis of Organic High-k Semiconductors Based on Spiro-Gridized Nanopolymers. *Research* **2022**, *2022*, 9820585, https://doi.org/10.34133/2022/9820585.
3. Wang, Y.; Huang, X.; Li, T.; Li, L.; Guo, X.; Jiang, P. Polymer-Based Gate Dielectrics for Organic Field-Effect Transistors. *Chem. Mater.* **2019**, *31*, 2212-2240, https://doi.org/10.1021/acs.chemmater.8b03904.
4. Xue, H.; Huang, P.-H.; Göthelid, M.; Strömberg, A.; Niklaus, F.; Li, J. Ultrahigh-Rate On-Paper PEDOT:PSS-Ti2C Microsupercapacitors with Large Areal Capacitance. *Adv. Funct. Mater.* **2024**, *34*, 2409210, https://doi.org/10.1002/adfm.202409210.
5. Nwaeze, G. Solution-Processed Conducting Films for Organic Field-Effect Transistors (OFETs). Master Thesis, The University of Manchester, United Kingdom, **22 July 2021**.
6. Abdullah, N.A.; Hussein, A.A.; Shabeeb, G.M.; Abdulelah, H. Evaluation of the Addition of O-Toluidine and Nano-Ag on The Optical and Electrical Properties of PEDOT-PSS Polymer. *Int. J. Sci. Adv.* **2025**, *6*, 563-570, https://doi.org/10.51542/ijscia.v6i3.23.
7. Choi, C.; Yun, T.G.; Hwang, B. Dispersion Stability of Carbon Nanotubes and Their Impact on Energy Storage Devices. *Inorganics* **2023**, *11*, 383, https://doi.org/10.3390/inorganics11100383.
8. Wu, F.; Liu, Y.; Zhang, J.; Duan, S.; Ji, D.; Yang, H. Recent Advances in High-Mobility and High-Stretchability Organic Field-Effect Transistors: From Materials, Devices to Applications. *Small Methods* **2021**, *5*, 2100676, https://doi.org/10.1002/smtd.202100676.
9. Zeinedini, A.; Akhavan-Safar, A.; da Silva, L.F.M. The role of agglomeration in the physical properties of CNTs/polymer nanocomposites: A literature review. *Proceedings of the Institution of Mechanical Engineers, Part L: Journal of Materials: Design and Applications* **2025**, 14644207251316470, https://doi.org/10.1177/14644207251316470.
10. Wang, Y.; Wustoni, S.; Surgailis, J.; Zhong, Y.; Koklu, A.; Inal, S. Designing organic mixed conductors for electrochemical transistor applications. *Nat. Rev. Mater.* **2024**, *9*, 249-265, https://doi.org/10.1038/s41578-024-00652-7.
11. Mesforush, S.; Cazorla, A.; Melville, H.; Blanchard, P.; Klauk, H.; Zschieschang, U.; Zhang, M.; Fijahi, L.; Mas-Torrent, M.; Barrena, E. Gate-Dielectric Surface Engineering With Fluorinated Monolayers: Minimizing Contact Resistance and Nonidealities in OFETs. *Adv. Electron. Mater.* **2025**, e00260, https://doi.org/10.1002/aelm.202500260.
12. Wu, X.; Zhu, X.; Sun, L.; Zhang, S.; Ren, Y.; Wang, Z.; Zhang, X.; Yang, F.; Zhang, H.-L.; Hu, W. Navigating the transitional window for organic semiconductor single crystals towards practical integration: from materials, crystallization, and technologies to real-world applications. *Chem. Soc. Rev.* **2025**, *54*, 1699-1732, https://doi.org/10.1039/D4CS00987H.
13. Balu, S.; Ganapathy, D.; Arya, S.; Atchudan, R.; Sundramoorthy, A.K. Advanced photocatalytic materials based degradation of micropollutants and their use in hydrogen production – a review. *RSC Adv.* **2024**, *14*, 14392-14424, https://doi.org/10.1039/D4RA01307G.
14. Goffri, S.; Müller, C.; Stingelin-Stutzmann, N.; Breiby, D.W.; Radano, C.P.; Andreasen, J.W.; Thompson, R.; Janssen, R.A.J.; Nielsen, M.M.; Smith, P.; Sirringhaus, H. Multicomponent semiconducting polymer systems with low crystallization-induced percolation threshold. *Nat. Mater.* **2006**, *5*, 950-956, https://doi.org/10.1038/nmat1779.
15. Lukyanov, D.A.; Levin, O.V. Inkjet Printing with (Semi)conductive Conjugated Polymers: A Review. *ChemEngineering* **2024**, *8*, 53, https://doi.org/10.3390/chemengineering8030053.
16. Zhu, G.; Zhao, Y.; Liu, Y. Overview of electrohydrodynamic deposition for fabricating organic thin film transistors. *J. Mater. Chem. C* **2024**, *12*, 14222-14245, https://doi.org/10.1039/D4TC02302A.
17. Yusof, N.S.; Mohamed, M.F.P.; Ghazali, N.A.; Ishak, M.K.; Shaari, S. Direct-Written Silver Electrodes for All-Solution-Processed Low-Voltage Organic Thin Film Transistors Towards Flexible Electronics Applications. *J. Adv. Res. Micro Nano Eng.* **2024**, *21*, 75-88, https://doi.org/10.37934/armne.21.1.7588.
18. Kong, M.; Yang, M.; Li, R.; Long, Y.-Z.; Zhang, J.; Huang, X.; Cui, X.; Zhang, Y.; Said, Z.; Li, C. Graphene-based flexible wearable sensors: mechanisms, challenges, and future directions. *Int. J. Adv. Manuf. Technol.* **2024**, *131*, 3205-3237, https://doi.org/10.1007/s00170-023-12007-7.
19. Sabet, M. Advanced Functionalization Strategies for Carbon Nanotube Polymer Composites: Achieving Superior Dispersion and Compatibility. *Polym. Technol. Mater.* **2025**, *64*, 465-494, https://doi.org/10.1080/25740881.2024.2409312.

20. Sun, M.; Wang, S.; Liang, Y.; Wang, C.; Zhang, Y.; Liu, H.; Zhang, Y.; Han, L. Flexible Graphene Field-Effect Transistors and Their Application in Flexible Biomedical Sensing. *Nano-Micro Lett.* **2024**, *17*, 34, https://doi.org/10.1007/s40820-024-01534-x.
21. Rajab, M.Z.; Ziadan, K.M.; Al-Attar, H.A. The effect of solvent (NMP, DMSO) on the electronic transition of nano blend POT: (PEDOT: PSS/MWCNT). *AIP Conf. Proc.* **2022**, *2660*, 020068, https://doi.org/10.1063/5.0107874.
22. Lu, L.; Wang, D.; Pu, C.; Cao, Y.; Li, Y.; Xu, P.; Chen, X.; Liu, C.; Liang, S.; Suo, L.; Cui, Y.; Zhao, Z.; Guo, Y.; Liang, J.; Liu, Y. High-performance flexible organic field effect transistors with print-based nanowires. *Microsyst. Nanoeng.* **2023**, *9*, 80, https://doi.org/10.1038/s41378-023-00551-x.
23. Ghosh, P.; Datta, K.; Mulchandani, A.; Han, S.-H.; Koinkar, P.; Shirsat, M.D. Poly(o-toluidine) Nanowires Based Organic Field Effect Transistors: A Study on Influence of Anionic Size of Dopants and SWNTs as a Dopant. *J. Phys. Chem. C* **2013**, *117*, 15414-15420, https://doi.org/10.1021/jp404674j.
24. Biswas, M.; Dey, A.; Sarkar, S.K. Polyaniline Based Field Effect Transistor for Humidity Sensor. *Silicon* **2022**, *14*, 8919-8925, https://doi.org/10.1007/s12633-021-01594-3.
25. Fan, S.; Vu, Q.A.; Lee, S.; Phan, T.L.; Han, G.; Kim, Y.-M.; Yu, W.J.; Lee, Y.H. Tunable Negative Differential Resistance in van der Waals Heterostructures at Room Temperature by Tailoring the Interface. *ACS Nano* **2019**, *13*, 8193-8201, https://doi.org/10.1021/acsnano.9b03342.

Publisher's Note & Disclaimer